

# Low-fidelity DNA synthesis by the L979F mutator derivative of *Saccharomyces cerevisiae* DNA polymerase $\zeta$

Jana E. Stone<sup>1</sup>, Grace E. Kissling<sup>2</sup>, Scott A. Lujan<sup>1</sup>, Igor B. Rogozin<sup>3</sup>, Carrie M. Stith<sup>4</sup>, Peter M. J. Burgers<sup>4</sup> and Thomas A. Kunkel<sup>1,\*</sup>

<sup>1</sup>Laboratory of Molecular Genetics and Laboratory of Structural Biology, <sup>2</sup>Biostatistics Branch, National Institute of Environmental Health Sciences Research, NIH, DHHS, Research Triangle Park, NC 27709, <sup>3</sup>National Center for Biotechnology Information, National Library of Medicine, NIH, DHHS, Bethesda, MD 20894 and <sup>4</sup>Department of Biochemistry and Molecular Biophysics, Washington University School of Medicine, St. Louis, MO 63110, USA

Received February 11, 2009; Revised March 26, 2009; Accepted March 30, 2009

## ABSTRACT

To probe Pol  $\zeta$  functions *in vivo* via its error signature, here we report the properties of *Saccharomyces cerevisiae* Pol  $\zeta$  in which phenylalanine was substituted for the conserved Leu-979 in the catalytic (Rev3) subunit. We show that purified L979F Pol  $\zeta$  is 30% as active as wild-type Pol  $\zeta$  when replicating undamaged DNA. L979F Pol  $\zeta$  shares with wild-type Pol  $\zeta$  the ability to perform moderately processive DNA synthesis. When copying undamaged DNA, L979F Pol  $\zeta$  is error-prone compared to wild-type Pol  $\zeta$ , providing a biochemical rationale for the observed mutator phenotype of *rev3-L979F* yeast strains. Errors generated by L979F Pol  $\zeta$  *in vitro* include single-base insertions, deletions and substitutions, with the highest error rates involving stable misincorporation of dAMP and dGMP. L979F Pol  $\zeta$  also generates multiple errors in close proximity to each other. The frequency of these events far exceeds that expected for independent single changes, indicating that the first error increases the probability of additional errors within 10 nucleotides. Thus L979F Pol  $\zeta$ , and perhaps wild-type Pol  $\zeta$ , which also generates clustered mutations at a lower but significant rate, performs short patches of processive, error-prone DNA synthesis. This may explain the origin of some multiple clustered mutations observed *in vivo*.

## INTRODUCTION

DNA polymerase  $\zeta$  (Pol  $\zeta$ ) has a significant role in a variety of replication processes that contribute to mutagenesis

(1,2). The catalytic subunit of Pol  $\zeta$  is encoded by *REV3*. A second subunit, encoded by *REV7*, is also essential for the catalytic activity of Pol  $\zeta$ . *REV3* and *REV7* were initially identified in screens for *Saccharomyces cerevisiae* mutants that have reduced frequencies of mutagenesis resulting from exposure to ultraviolet (UV) light (3–5). Pol  $\zeta$  was subsequently implicated in damage-induced mutagenesis resulting from exposure to additional DNA damaging agents, including those that cause oxidative and alkylation damage (1). These studies suggested that Pol  $\zeta$  is a low-fidelity polymerase that is involved in translesion DNA synthesis (TLS). Deletion of *REV3* or *REV7* in yeast reduces the rate of spontaneous mutation by half or more (1,6–9). This implies that DNA synthesis by Pol  $\zeta$  is required for the majority of spontaneous mutagenesis, presumably due to TLS past endogenous DNA damage. Pol  $\zeta$  has also been implicated in multiple DNA processing pathways, including double-strand break repair (10,11), interstrand crosslink repair (12,13) and somatic hypermutation to diversify immunoglobulin genes (14,15).

Pol  $\zeta$  is a member of the B family of DNA polymerases based on homology, but differs from other eukaryotic family members in several ways. Unlike Pol  $\delta$  and Pol  $\epsilon$ , but like Pol  $\alpha$ , Pol  $\zeta$  lacks a 3' exonuclease proofreading activity. When copying undamaged templates *in vitro*, the Pol  $\zeta$  error rate for insertion-deletion errors is similar to that of the other exonuclease-deficient B family members, while its base substitution fidelity is somewhat lower (16). DNA synthesis by Pol  $\zeta$  *in vitro* is unique in that it generates multiple, closely-spaced sequence changes at higher rates than have been observed for other DNA polymerases (16). Interestingly, complex mutants are also a feature of Pol  $\zeta$ -dependent mutational spectra *in vivo* (6,7,17–19). Pol  $\zeta$  has high activity and fidelity for the bypass of some lesions, such as thymine glycol (20),

\*To whom correspondence should be addressed. Tel: +1 919 541 2644; Fax: +1 919 541 7613; Email: kunkel@niehs.nih.gov

while it has low activity for the bypass of other lesions, such as *cis-syn* cyclobutane pyrimidine dimers (CPDs) (21). Pol  $\zeta$  is also promiscuous in extending mismatched and/or damaged primer termini (22–27). This property has led to the suggestion that the primary role of Pol  $\zeta$  is to extend mismatched or aberrant primer termini generated when other DNA polymerases insert nucleotides opposite lesions (1,22,28,29).

Toward the goal of understanding the contributions of Pol  $\zeta$  and the other B family polymerases to mutagenesis *in vivo*, we have been identifying and characterizing mutant polymerases that retain high catalytic activity but have reduced DNA synthesis fidelity and an error signature that is distinctive enough to track polymerase functions *in vivo*. The most informative missense alleles have been obtained by mutating residues homologous to Leu-415 in bacteriophage RB69 Pol, a B family member. In the crystal structure of RB69 Pol, Leu-415 is located adjacent to Tyr-416, a residue in the nascent base-pair binding pocket of the polymerase active site that contacts the incoming dNTP (30). Substitutions for RB69 Pol Leu-415 and equivalent residues in bacteriophage T4 pol and yeast Pol  $\alpha$ , Pol  $\delta$  and Pol  $\epsilon$  result in mutant polymerases that have reduced fidelity while retaining robust catalytic activity (31–40). In family A polymerases, mutating the equivalent isoleucine residue in the polymerase active sites of *Escherichia coli* pol I and *Thermus aquaticus* pol I also reduces fidelity (41,42). Substitutions to the conserved leucine residue in B family polymerases can also affect the TLS activity. L868F Pol  $\alpha$  has an elevated capacity for TLS past CPDs, 6-4 photoproducts and apurinic and apyrimidinic (AP) sites (37) and L415F RB69 pol has elevated ability to insert nucleotides opposite AP sites and 8-oxo-guanine (38). In Pol  $\eta$ , which is member of the Y family of low-fidelity TLS polymerases, the residue equivalent to RB69 Pol Leu-415 is Phe-34. When leucine is substituted for Phe-34, Pol  $\eta$  has reduced TLS activity *in vitro* (37). Collectively, these studies suggest that the presence of a phenylalanine at this location in the polymerase active site is particularly important for DNA synthesis fidelity and for TLS.

Previously, we analyzed six substitutions for *S. cerevisiae* Rev3 residue Leu-979, the Pol  $\zeta$  residue that is homologous to RB69 Pol Leu-415. We found that yeast strains in which phenylalanine or methionine had been substituted for Leu-979 retained nearly wild-type survival following exposure to UV, while the frequency of UV-induced mutations was elevated (43). UV-induced mutagenesis was particularly high in *rev3-L979F rad30 $\Delta$*  double mutants, which lack TLS by Pol  $\eta$ . These data suggested that L979F Pol  $\zeta$  retains catalytic activity and the ability to participate in mutagenic bypass of UV photoproducts. In addition, spontaneous mutation rates were elevated in *rev3-L979F* and *rev3-L979F rad30 $\Delta$*  mutant strains (43), implying that the phenylalanine substitution reduces the fidelity of DNA synthesis by Pol  $\zeta$ . Here we test this possibility by measuring the activity, processivity, fidelity and error specificity of L979F Pol  $\zeta$  *in vitro*. The results reveal an unprecedented ability to generate clustered sequence changes that likely result from processive patches of highly error-prone DNA

synthesis, an error signature that may be useful for monitoring Pol  $\zeta$  functions *in vivo*.

## MATERIALS AND METHODS

### Enzymes

Two-subunit *S. cerevisiae* Pol  $\zeta$  (Rev3-Rev7) and L979F Pol  $\zeta$  (Rev3<sup>L979F</sup>-Rev7) were expressed in yeast and purified as previously described (44). Three-subunit *S. cerevisiae* Pol  $\delta$  was expressed in yeast and purified as previously described (45). *S. cerevisiae* RPA, RFC1 $\Delta$ -5 and PCNA were expressed in *E. coli* and purified as previously described (46,47).

### Measuring polymerase specific activity and processivity

Polymerase specific activity was measured using activated calf thymus DNA as previously described (36). Processivity measurements were performed as described previously (48). The template strand was a 70-mer of *lacZ* sequence with a 5' biotin moiety (5'-ATGACCATGATTACGAATTCCAGCTCGGTACCGGGTTGACCTTTGGAGTCGACCTGCAGAAATTCACCTGG). Two primers were annealed to this template: BP14 (5'-CCAGTGAATTTCTG) with a 5' biotin moiety and <sup>32</sup>P-labeled LP16 (5'-CAGGTCGACTCCAAAG), which did not have a 5' biotin moiety. Substrate ends were blocked with streptavidin (Roche) before use, as described (48). Each reaction mixture (30  $\mu$ l) contained 40 mM Tris-HCl (pH 7.8), 8 mM MgAc<sub>2</sub>, 100 mM NaCl, 1 mM ATP, 100  $\mu$ M of each dNTP, 200  $\mu$ g/ml BSA, 1 pmol DNA substrate and 120 fmol wild-type Pol  $\zeta$  or 200 fmol L979F Pol  $\zeta$ . Where indicated, 1.2 pmol each of PCNA, RFC and RPA were added. All components except the polymerase were mixed on ice and then incubated at 30 C for 2 min. Polymerase was added to start reactions, and samples were removed at indicated times and added to an equal volume of formamide loading buffer (95% deionized formamide, 25 mM EDTA, 0.01% bromophenol blue and 0.01% xylene cyanol) to stop the reaction. Reactions were performed in duplicate. Samples were analyzed in 12% denaturing polyacrylamide gels. Products were quantified and polymerization parameters were calculated as previously described (48).

### Fidelity measurements

The fidelity of DNA synthesis was measured as previously described (16). Polymerization reactions were performed using gapped M13mp2 DNA substrates containing the *lacZ $\alpha$* -complementation gene sequence as a template in either the transcribed, forward (+ strand) or reverse (- strand) orientation. In order to simplify the preparation of gapped substrates, the forward (+) and reverse (-) substrates used here were slightly modified from those described previously (16). PvuII sites were introduced into each substrate by site-directed mutagenesis at M13mp2 positions 5822–5827 and 5886–5891 using mutagenic oligonucleotides and T7 DNA polymerase (49). Gapped substrates were then prepared as described (50) to create 343-nucleotide single-stranded gaps. Gap-filling

reaction mixtures (25  $\mu$ l) contained 20 mM Tris-HCl (pH 7.7), 8 mM MgAc<sub>2</sub>, 60 mM NaCl, 0.5 mM ATP, 100  $\mu$ M of each dNTP, 1 mM DTT, 100  $\mu$ g/ml bovine serum albumin, 0.1% Triton X-100,  $\sim$ 1 pmol Pol  $\zeta$  or L979F Pol  $\zeta$ , 500 fmol PCNA, 200 fmol RFC, 5 pmol RPA and 25 fmol (1 nM) of gapped DNA substrate. Polymerization reactions were incubated at 30  $^{\circ}$ C for 30 min. Examination of products by agarose gel electrophoresis as previously described (50) revealed that all reactions filled the gap (data not shown). DNA products of gap-filling reactions were introduced into *E. coli* and plated as described previously to score blue M13 plaques (no detectable mutations) and light-blue or colorless plaques resulting from DNA synthesis errors (50). The types of errors were determined by sequencing the *lacZ* $\alpha$ -complementation gene from single-stranded M13 DNA isolated from independent mutant plaques using primer SNM43 (5'-CGCGTTAAATTTTGTAAATCAGCTG). Due to the position of this primer, sequence data were generated for 322 of the 343 nucleotides present within the gap. The sequenced region includes all of the *lacZ* sequence and lacks only the initial 21 nucleotides of M13mp2 sequence.

As previously described (16), the error rates (ER) for phenotypically detectable mutations were calculated with the equation  $ER = [(N_i/N) \times F]/(D \times 0.6)$ , where  $N_i$  is the number of mutations of a particular type,  $N$  is number of plaques sequenced,  $F$  is the mutant frequency,  $D$  is number of detectable sites for the given mutation type and 0.6 is the probability of expressing a mutant allele in *E. coli* (determined experimentally). The error rates for phenotypically undetectable mutations were calculated as  $ER = N_i/(b \times N)$ , where  $b$  is the number of the times the template base is observed in the sequenced region. As it is not possible to calculate an error rate for events that involve multiple nucleotides over variable distances, error frequencies (EF) were calculated for complex mutations and tandem base substitutions using the following equation:  $EF = (N_i/N) \times F$ .

### Statistical analyses

Differences between error rates were determined using two-tailed Chi-square analyses. For each type of mutation, the two values used in Chi-square analyses were the number of mutant plaques observed with that mutation type and the number of plaques of all other types ( $N_{\text{not } i}$ ) expected based on the error rate, which were calculated as  $N_{\text{not } i} = (N_i/ER) - N_i$ . For example, to test if wild-type Pol  $\zeta$  and L979F Pol  $\zeta$  made G $\cdot$ dGMP errors at significantly different rates, values for  $N_{G \cdot dGMP}$  and  $N_{\text{not } G \cdot dGMP}$  generated by wild-type Pol  $\zeta$  were tested against values for  $N_{G \cdot dGMP}$  and  $N_{\text{not } G \cdot dGMP}$  generated by L979F Pol  $\zeta$ . When multiple tests were performed, the Bonferroni correction was applied using  $\alpha = 0.05$ . Fisher exact tests were used to compare differences between the number of insertion/deletions and base substitutions in complex mutations versus those identified as single mutations. Binomial probabilities were used to identify mutation hotspots in the mutation spectra via two methods. The first method has been previously

described (51,52). The second, less conservative method is described in the Supplementary Data.

## RESULTS

### Purity and specific activity of L979F Pol $\zeta$

Wild-type and L979F Pol  $\zeta$  were expressed in yeast and purified as previously described (44). Each preparation contained two major polypeptides whose masses correspond to Rev3 and Rev7 (Figure 1A), indicating that substituting phenylalanine for Leu-979 does not interfere with the ability of Rev3 to interact with Rev7. The two enzyme preparations were of high and comparable purity (Figure 1A) and neither preparation contained detectable exonuclease activity (data not shown). Using activated calf thymus DNA as a substrate, the specific activity of L979F Pol  $\zeta$  was about 3-fold lower than that of wild-type Pol  $\zeta$  (Figure 1B). Both forms of Pol  $\zeta$  have substantially lower specific activity than three-subunit yeast Pol  $\delta$ , which has a major role in chromosomal DNA replication.

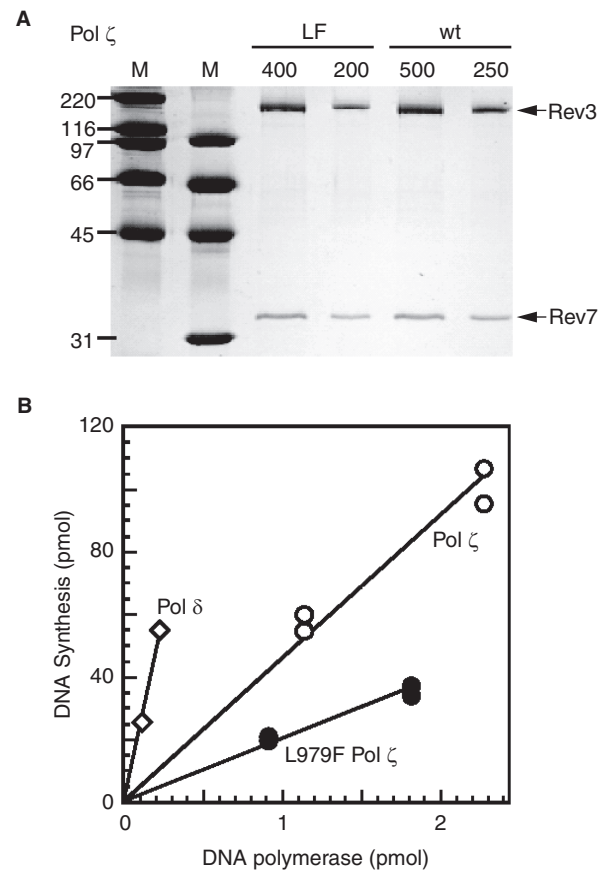


**Figure 1.** Purity and polymerase specific activity of purified L979F Pol  $\zeta$  and wild-type Pol  $\zeta$ . (A) Purified wild-type L979F Pol  $\zeta$  (LF) and Pol  $\zeta$  (wt). Samples of wild-type Pol  $\zeta$  (500 and 250  $\mu$ g) and of L979F Pol  $\zeta$  (400 and 200  $\mu$ g) were analyzed on an SDS-PAGE gel and stained with colloidal coomassie. Lanes marked M show molecular weight markers of the indicated sizes. (B) Polymerase specific activity. Activated calf thymus DNA was used as a substrate to measure the catalytic activity of Pol  $\zeta$  and L979F Pol  $\zeta$ . Yeast Pol  $\delta$  was used for comparison.

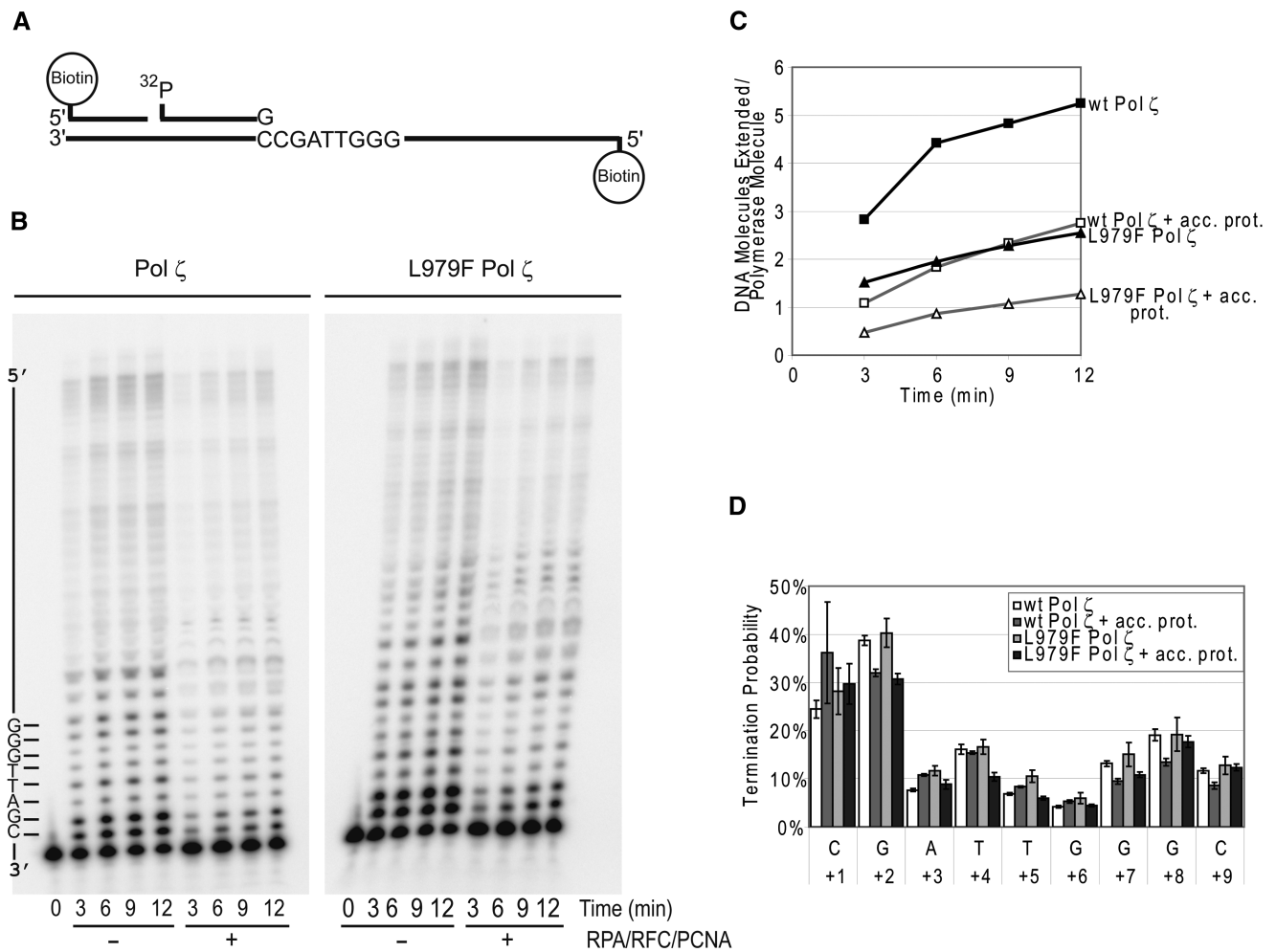


**Figure 2.** Catalytic activity of wild-type and L979F Pol ζ. (A) Substrate. The substrate consists of a 70-mer template oligonucleotide with a 5'-biotin moiety, to which were annealed a 14-bp oligonucleotide with a 5' biotin moiety and a <sup>32</sup>P-labeled 16-bp primer without a biotin moiety. Streptavidin was used to block substrate ends. (B) Primer extension assay. Eight- and five-fold excess substrate over enzyme were used for wild-type Pol ζ and L979F Pol ζ, respectively. Under these conditions, each substrate molecule is encountered by a polymerase molecule only once. Where indicated, PCNA, RFC and RPA were loaded onto the substrate and incubated for 2 min, and then polymerase was added to start the reactions. Time points were taken at 3, 6, 9 and 12 min. A portion of the template sequence is shown at the left. (C) Primer extension activity. The number of DNA molecules extended per polymerase molecule is plotted against time. Acc. prot. indicates presence of accessory proteins PCNA, RFC and RPA. (D) Termination probabilities at each template position. The termination probabilities shown are an average of the four time points shown in (B), with the error bars indicating the standard deviations between the time points.

### Processivity of L979F Pol ζ

We examined the ability of wild-type Pol ζ and L979F Pol ζ to copy an undamaged oligonucleotide primer-template containing 40 nucleotides of single-stranded DNA template (Figure 2A). This substrate was present in sufficient excess over Pol ζ such that DNA products reflect a single cycle of processive synthesis. Under this condition, wild-type Pol ζ primarily incorporated 1–10 nucleotides (Figure 2B, left), with a small proportion of products reflecting processive synthesis to the end of the template. The time-dependent accumulation of DNA products in excess over the amount of polymerase used (Figure 2B and C) indicates that at least some Pol ζ molecules dissociate after synthesis and cycle to previously unused primers. As is expected for synthesis by Pol ζ (1), the probabilities for termination of processive synthesis

are highest for the first two incorporation events (Figure 2D, open bars). After the first two incorporation events, Pol ζ is slightly more processive, because the probabilities of termination drop from 30% to 40% for template positions +1 and +2 to 5–20% for template positions +2 through +9 (Figure 2D). We then tested activity of Pol ζ in the presence of proliferating cell nuclear antigen (PCNA), replication factor C (RFC) and replication protein A (RPA). The accessory proteins used in these experiments are preparations that have previously been shown to be active and can stimulate DNA synthesis by yeast Pol δ (see Figure 1 in ref. 53). With this undamaged primer-template, whose ends were blocked with streptavidin, the inclusion of the accessory proteins had little effect on the processivity (Figure 2B) or termination probability (Figure 2D) of the wild-type Pol ζ

**Table 1.** Fidelity of Pol  $\zeta$  and L979F Pol  $\zeta$  in the presence of accessory proteins PCNA, RFC and RPA

	Pol $\zeta$		L979F Pol $\zeta$	
	FWD (+) strand	REV (-) strand	FWD (+) strand	REV (-) strand
Total plaques	7359	7414	7072	4567
<i>lacZ</i> mutants	131	210	609	635
Mutant frequency	0.018	0.028	0.086	0.14
Number of mutants sequenced	90	96	106	115
Error Rates ( $\times 10^{-5}$ )				
Frameshifts				
-1	0.96 (6)	1.6 (7)	3.9 (6)	3.9 (4)
+1	0.48 (3)	0.47 (2)	4.6 (7)	5.9 (6)
Base substitutions				
Detectable	16 (79)	25 (84)	77 (93)	146 (118)
Undetectable	52 (15)	45 (14)	300 (101)	460 (169)
Frequency of tandem double base substitutions	0.0002 (1)	$\leq 0.0003$ (0)	0.0089 (11)	0.0097 (8)
Frequency of complex mutations	0.0002 (1)	0.0009 (3)	0.058 (71)	0.14 (112)

Error rates for phenotypically detectable mutations and undetectable changes were calculated as described in Materials and Methods section. Numbers in parenthesis represent the number of times the mutation event was observed. Complex mutations are defined as multiple mutations that occurred with nine or fewer intervening bases, excluding tandem double base substitutions. Both detectable and undetectable mutations were included in tandem base substitutions and complex categories. The single-base substitutions or frameshifts observed within the tandem base substitutions and complex mutations were not used in the error rate calculations of single-base substitutions or frameshifts.

heterodimer. The accessory proteins did decrease primer utilization by about two-fold (Figure 2B and C), suggesting that the accessory proteins may inhibit cycling of Pol  $\zeta$  to new substrate molecules. These results are consistent with earlier observations on the effects of accessory proteins on Pol  $\zeta$  when copying undamaged DNA (see Figure 1B in ref. 44). The lack of an increase in wild-type Pol  $\zeta$  processivity upon addition of accessory proteins contrasts with the increased processivity observed when these same accessory proteins were included in reactions catalyzed by yeast Pol  $\delta$  (data not shown, for an earlier example see ref. 48). It should also be noted that preliminary experiments have indicated that the concentration of NaCl in the reaction can affect stimulation of Pol  $\zeta$  by the accessory proteins (Burgers *et al.*, unpublished results) and experiments to explore this effect are ongoing.

When parallel reactions were performed with L979F Pol  $\zeta$ , its processivity (Figure 2B) and site-specific termination probabilities (Figure 2D) were similar to those of wild-type Pol  $\zeta$ . However, the ability of L979F Pol  $\zeta$  to cycle between substrate molecules was reduced compared to wild-type Pol  $\zeta$  (Figure 2C). As with wild-type Pol  $\zeta$ , inclusion of the accessory proteins did not affect processivity or termination probability, and slightly decreased cycling. Overall, the results indicate that substituting phenylalanine for Leu-979 in yeast Pol  $\zeta$  slightly reduces specific activity and cycling behavior, but does not alter processivity, so that L979F Pol  $\zeta$  is capable of processive incorporation, in some instances of at least 40 nucleotides.

### Fidelity of L979F Pol $\zeta$

Towards the goal of using the *rev3-L979F* allele for functional studies *in vivo*, we determined the fidelity of L979F Pol  $\zeta$  when copying an undamaged *lacZ* complementation template sequence in gapped M13mp2 DNA. Parallel reactions were performed with substrates containing either the *lacZ* (+) strand template or the *lacZ* (-)

strand template. Because the composition and preparation of the gapped substrates used in this study differ slightly from those used in a previous study of the fidelity of wild-type yeast Pol  $\zeta$  (16, see Materials and Methods section), we use new data generated here with wild-type Pol  $\zeta$  for comparison to L979F Pol  $\zeta$ . Since the accessory proteins PCNA, RFC and RPA are known to interact with Pol  $\zeta$ , gap-filling reactions were performed in the presence of these proteins, in order to more closely mimic DNA synthesis by L979F Pol  $\zeta$  *in vivo*. Previous work suggested that the accessories had a minimal effect on the fidelity of wild-type Pol  $\zeta$  (16). In the presence of the accessory proteins, both wild type and L979F Pol  $\zeta$  completely filled the single-stranded gap in the (+) and (-) strand substrates (data not shown). The M13mp2 DNA products were scored for the frequency of colorless and light blue plaques, which reflect DNA synthesis errors, among a larger number of dark blue plaques resulting from correct DNA synthesis. The mutant frequencies generated by L979F Pol  $\zeta$  were 5-fold higher than those of wild-type Pol  $\zeta$  for both templates (Table 1), indicating that the phenylalanine substitution reduces the fidelity of DNA synthesis by yeast Pol  $\zeta$ . The mutant frequencies generated by both wild-type and L979F Pol  $\zeta$  were 1.6-fold higher for the (-) strand template versus the (+) strand template. Although small, this difference is statistically significant ( $P < 0.001$ ), consistent with sequence context-dependent differences in Pol  $\zeta$  fidelity when copying the complementary strands (see below).

To explore sequence context-dependent differences further and to define the error specificity of L979F Pol  $\zeta$ , we sequenced the *lacZ*-complementation gene and flanking M13mp2 sequences from collections of independent mutant plaques generated by wild-type and L979F Pol  $\zeta$ . Sequencing *lacZ* mutants from reactions performed by wild-type Pol  $\zeta$  revealed one, or sometimes two, sequence changes per mutant (Table 1). However, *lacZ* mutants

from reactions catalyzed by L979F Pol  $\zeta$  contained many more sequence changes per mutant (Table 1) and these were non-randomly distributed (Figure 3). To determine if more multiple mutations occurred more than would be expected based on the mutant frequency, the Poisson distribution was used to predict the expected number of *lacZ* mutants with two, three and four or more mutations, as described by Drake *et al.* (54). Wild-type Pol  $\zeta$  exceeded the prediction for *lacZ* mutants containing two or more detectable mutations for the (–) strand template but not the (+) strand template (Supplementary Table 1), while L979F Pol  $\zeta$  significantly exceeded the prediction for both templates (Supplementary Table 1). In addition, at least one silent hitchhiker mutation was observed in 94% of *lacZ* mutants generated by L979F Pol  $\zeta$ , while 15% of *lacZ* mutants generated by wild-type Pol  $\zeta$  contained a hitchhiker mutation (Supplementary Table 1). Based on the types, number and distribution of sequence changes observed, we placed errors into four classes: single-base deletions, single-base additions, single-base substitutions and more complex errors containing two or more closely-spaced sequence changes within nine nucleotides of each other (rationale explained below). Using the mutant frequencies and the proportions of each type of mutation, we calculated (see Materials and Methods section) error rates per nucleotide incorporated by wild-type and L979F Pol  $\zeta$  (Table 1). Due to the diversity in composition and spacing of sequence changes among the complex errors, we express these events as error frequencies rather than rates (Table 1).

#### Single-base insertion and deletion error rates of L979F Pol $\zeta$

Consistent with our earlier study (16), wild-type Pol  $\zeta$  generates single-base deletions and insertions at rates of about  $10^{-5}$  (Table 1), which is similar to the insertion-deletion error rates of other exonuclease-deficient B family enzymes (see Table 2 in ref. 16). In comparison, the single-base deletion error rates of L979F Pol  $\zeta$  were 4-fold and 2-fold higher than those of wild-type Pol  $\zeta$  for the (+) strand and (–) strand templates, respectively (Table 1). Thus, substituting phenylalanine for Leu-979 at the Pol  $\zeta$  active site modestly increases the rate at which deletion errors arise from misaligned intermediates with an extra base in the template strand. L979F Pol  $\zeta$  error rates for single-base insertions were similar to those for single-base deletions (Table 1). This contrasts with most other polymerases, which generate deletions at substantially higher rates than additions (55). Moreover, the rates of single-base insertions generated by L979F Pol  $\zeta$  were 10-fold and 12-fold higher than for wild-type Pol  $\zeta$  in the (+) and (–) strand templates, respectively (Table 1). Thus, substituting phenylalanine for Leu-979 at the Pol  $\zeta$  active site substantially increases the rate of addition errors involving misaligned intermediates with an extra base in the primer strand. Note that the effect of the L979F change on insertion-deletion formation by Pol  $\zeta$  is greater than indicated by these single-base rates, because the majority of insertions and deletions were

observed among the changes present in the complex mutations discussed below.

#### Base substitution error rates of L979F Pol $\zeta$

As observed in our previous study of wild-type Pol  $\zeta$  (16), the majority of errors committed by both wild-type and L979F Pol  $\zeta$  involve base-base mismatches that result in single-base substitutions (Table 1). L979F Pol  $\zeta$  also generated tandem double base substitutions at a frequency of about 0.9% (Table 1), a value that is much higher than for other B family members. The single-base substitutions were distributed throughout the (+) strand and (–) strand templates (Supplementary Figure 2) and reflect formation of all 12 mismatches (black bars in Figure 4A and B). This includes an unusually high rate of G•dGMP mismatches relative to other mismatches, as well as formation of C•dCMP mismatches, which are rarely generated by most other DNA polymerases. The data for wild-type Pol  $\zeta$  are the baseline against which we compared L979F Pol  $\zeta$ . L979F Pol  $\zeta$  generated a variety of substitutions that were distributed widely but non-randomly along both the (+) strand and (–) strand templates (Supplementary Figure 3). When overall base substitution error rates were calculated for L979F Pol  $\zeta$ , they were about 5-fold higher than for wild-type Pol  $\zeta$  for detectable base substitutions and 6–10-fold higher for silent base substitutions (Table 1). We then calculated rates for each of the 12 different single-base-base mismatches. We considered the data for the (+) strand template and the (–) strand template separately, in order to determine possible effects of sequence context on Pol  $\zeta$  fidelity as each of the two template bases of complementary base pairs was copied (Figure 4 and Supplementary Figure 1). L979F Pol  $\zeta$  generated error rates that were higher than for wild-type Pol  $\zeta$  by factors ranging from 2-fold to 75-fold (compare black and gray bars in Figure 4A and B). With both templates, L979F Pol  $\zeta$  significantly elevated the rates of phenotypically detectable A•dAMP, G•dAMP, A•dGMP and T•dGMP mismatches (Figure 4A and B), each of which involve misincorporation of purine precursors. For silent base-substitutions, the rates of A•dAMP, A•dGMP and T•dGMP mismatches were also significantly elevated by L979F Pol  $\zeta$  for both templates (Supplementary Figure 1A and B). Curiously, with both templates, the L979F replacement reduced the error rate for C•dCMP mismatches (Figure 4A and B, Supplementary Figure 1A and B). As a consequence, L979F Pol  $\zeta$  has a very strong bias for creating G•dGMP over C•dCMP mismatches, the two mistakes that could lead to a G:C to C:G transversion *in vivo*. Biases in error rates were also observed for certain other pairs of complementary mismatches, with the extent of the bias varying from none (e.g. gray bars in Figure 4A and B for C•dTTP versus G•dAMP), to  $\geq 18$ -fold (e.g. Figure 4A for A•dGMP versus T•dCMP).

#### Complex errors generated by L979F Pol $\zeta$

We reported earlier that wild-type yeast Pol  $\zeta$  generates *lacZ* mutants containing several single-base errors clustered within short patches at a rate that had not previously been seen with other DNA polymerases (16).

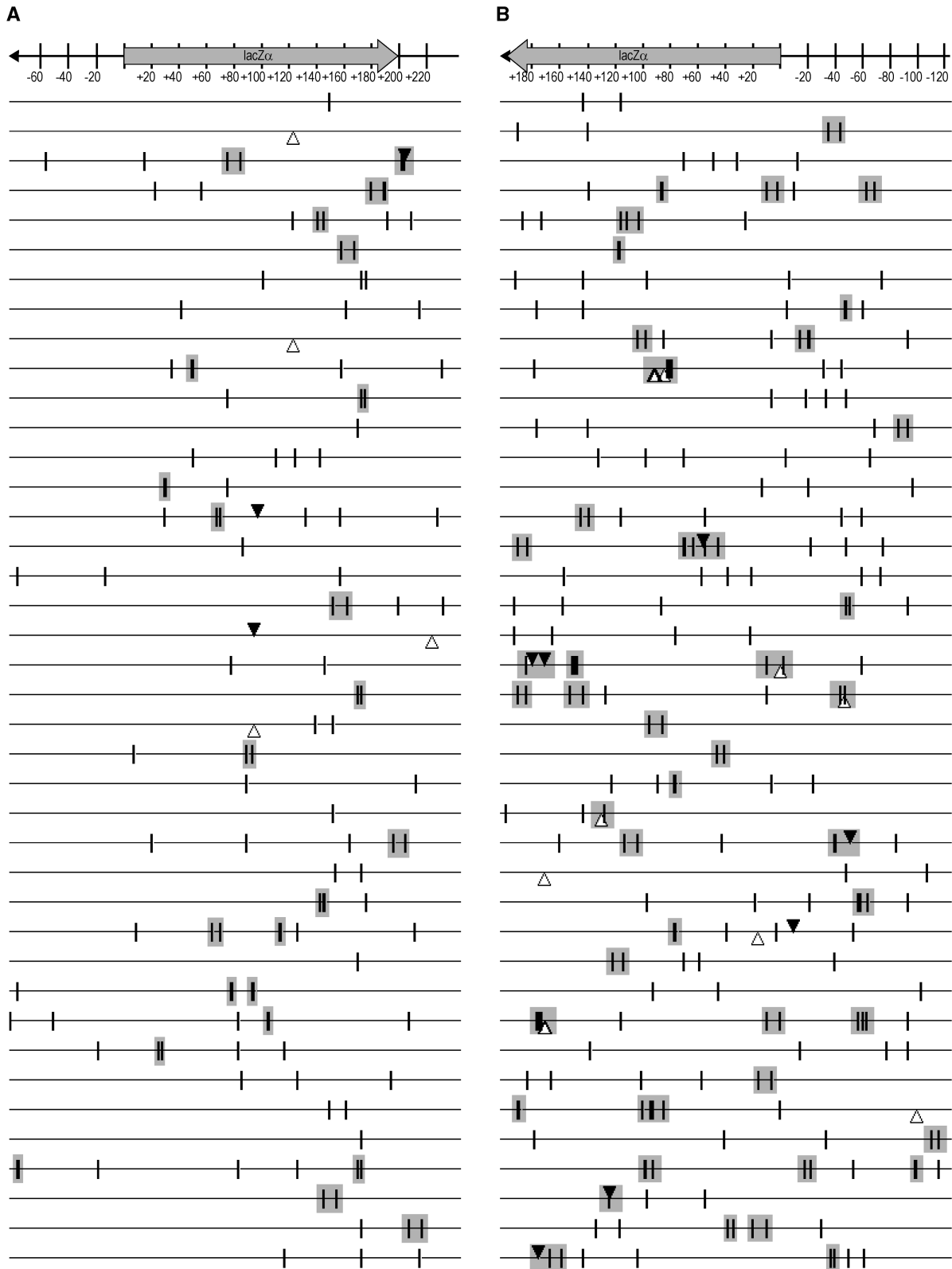


**Figure 3.** Alignment of mutations within *lacZ* mutants generated by L979F Pol  $\zeta$ . Alignment of a of sample sequences of *lacZ* mutants isolated from gap-filling reactions using (A) the (+) strand template and (B) the (-) strand template. The 40 sample sequences shown were the chosen at random. At top is a diagram showing the position of *lacZ* in the single-strand gapped region of M13mp2, which serves as the template for DNA synthesis. The direction of DNA synthesis is indicated with the arrowhead. Each horizontal line below the template diagram represents the sequence of one *lacZ* mutant. Mutations are indicated using pipe symbols for base substitutions, open triangles for -1 deletions and closed, inverted filled triangles for +1 insertions. Gray boxes indicate locations of complex mutations, which are defined as multiple mutations with nine or fewer intervening nucleotides.

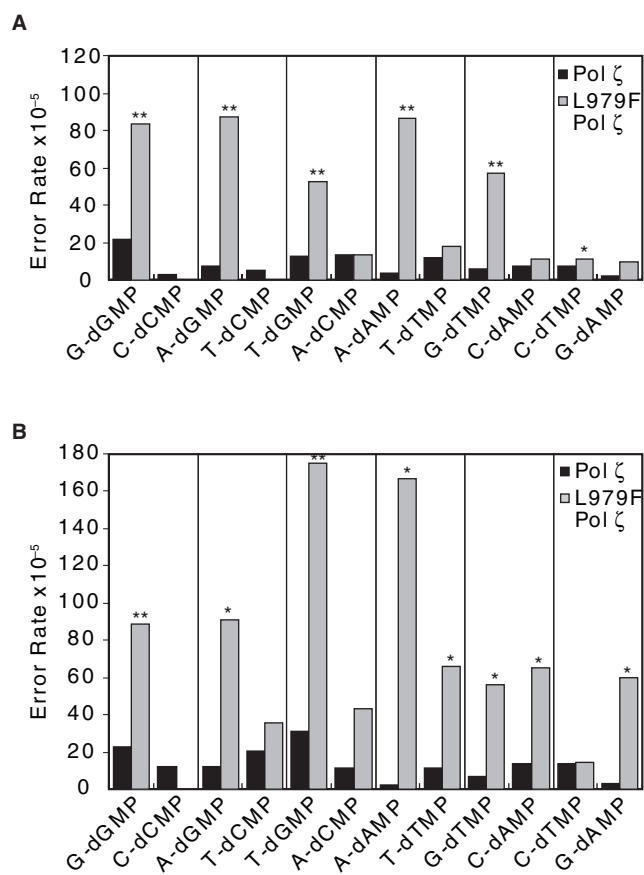


**Figure 4.** Base substitution error rates for wild-type Pol  $\zeta$  and L979F Pol  $\zeta$  in the presence of accessory proteins. Error rates for the 12 possible mismatches which generate base substitutions are shown for (A) the (+) strand template and (B) the (-) strand template. Only single, phenotypically detectable base substitutions were used to produce these graphs. See Supplementary Figure 1 for undetectable base substitutions. Each mismatch is shown paired with the complementary mismatch. Rate calculations were as described (16) and statistical tests were as described in Materials and Methods section. Single asterisks indicate mismatches which are made by L979F Pol  $\zeta$  significantly more often than by wild-type Pol  $\zeta$ . Double asterisks indicate mismatches which are made by L979F Pol  $\zeta$  significantly more often than by wild-type Pol  $\zeta$  and were made by L979F Pol  $\zeta$  significantly more often than the complementary mismatch.

In the present study, we again recovered a few such mutants from reactions catalyzed by wild-type Pol  $\zeta$  (Table 1 and Supplementary Table 2). Moreover, L979F Pol  $\zeta$  generated a large number of complex events (Table 1) scattered throughout the (+) and (-) strand templates (Figures 3 and 5 and Supplementary Table 2). Here we define complex mutations as clustered mutations with nine or fewer intervening nucleotides. This distance is based on structural data indicating that family B DNA polymerases interact with duplex primer-template for up to nine base pairs upstream of the polymerase active site (30). This distance is also based on the significant excess of adjacent mutations generated by L979F Pol  $\zeta$  that have 1–10 intervening nucleotides over the number predicted by Monte Carlo simulations (Figure 6). L979F Pol  $\zeta$  generated such complex mutations at very high frequencies, 0.058 for the (+) strand template and 0.14 for the (-) strand template (Table 1). These complex mutations

varied by template position, in the number of closely spaced mutations, in the spacing between mutations, and in the types of sequence changes (Figure 5 and Supplementary Table 2). At least one insertion or deletion was observed in 23% of the complex mutations generated by L979F Pol  $\zeta$  during replication of either template. As a result, the number of insertion-deletions observed within complex mutations significantly exceeded the number observed individually ( $P = 0.006$ ). Among the 12 possible base substitution errors, only A-to-C transversions were significantly over-represented within complex mutations compared to those observed individually ( $P < 0.0001$ , with detectable and undetectable mutations from both templates pooled). A-to-C transversions involving A•dGMP mismatches were also the first event in complex mutations more often than any other sequence change.

### Hotspots for mutations generated by L979F Pol $\zeta$

Assuming that a set of mutations are randomly distributed across the 322 nucleotides sequenced for each template, binomial probabilities can be used to determine the probability of observing several independent mutations at a particular location. Using a conservative approach, which has been previously described (51,52), four hotspots for single mutations were identified on the (+) strand template at positions at which five or more single mutations were created by L979F Pol  $\zeta$ . Similarly, three positions were identified on the (-) strand template where seven or more single mutations arose. In order to identify hotspots for complex errors, we applied binomial probabilities to the positions where the first mutation in each complex error occurred. Only complex events where the initial mutation occurs at a non-ambiguous position were used in this analysis. These analyses revealed that hotspots for complex errors generated by L979F Pol  $\zeta$  occurred when the first events in four or more complex mutations are located at the same position. Accordingly, hotspots for complex mutations generated by L979F Pol  $\zeta$  were identified at three positions on the (+) strand template and three positions on the (-) strand template (Figure 5 and Supplementary Figure 3). When a less conservative approach for identifying hotspots was used (described in the Supplementary Data), one additional hotspot for single mutations was identified on the (+) strand template and on the (-) strand template, an additional 10 hotspots for single mutations and one hotspot for complex events were identified. When the more conservative approach was applied, the template base is an A at six of the seven hotspots for single mutations and all of the hotspots for complex mutations (Figure 5 and Supplementary Figure 3). Of the six hotspots for complex mutations identified using the more conservative method, two occurred at positions that were also hotspots for single mutations. The strongest of these dual hotspots is at position 176 on the (+) strand template, where single A-to-C transversions occur at a rate of  $3 \times 10^{-3}$  and complex mutations that initiate with A-to-C transversions occur at a frequency of  $6 \times 10^{-3}$  (Figure 5). Because not every hotspot for single mutations is also a hotspot for complex mutations, nor is every hotspot for complex mutations also



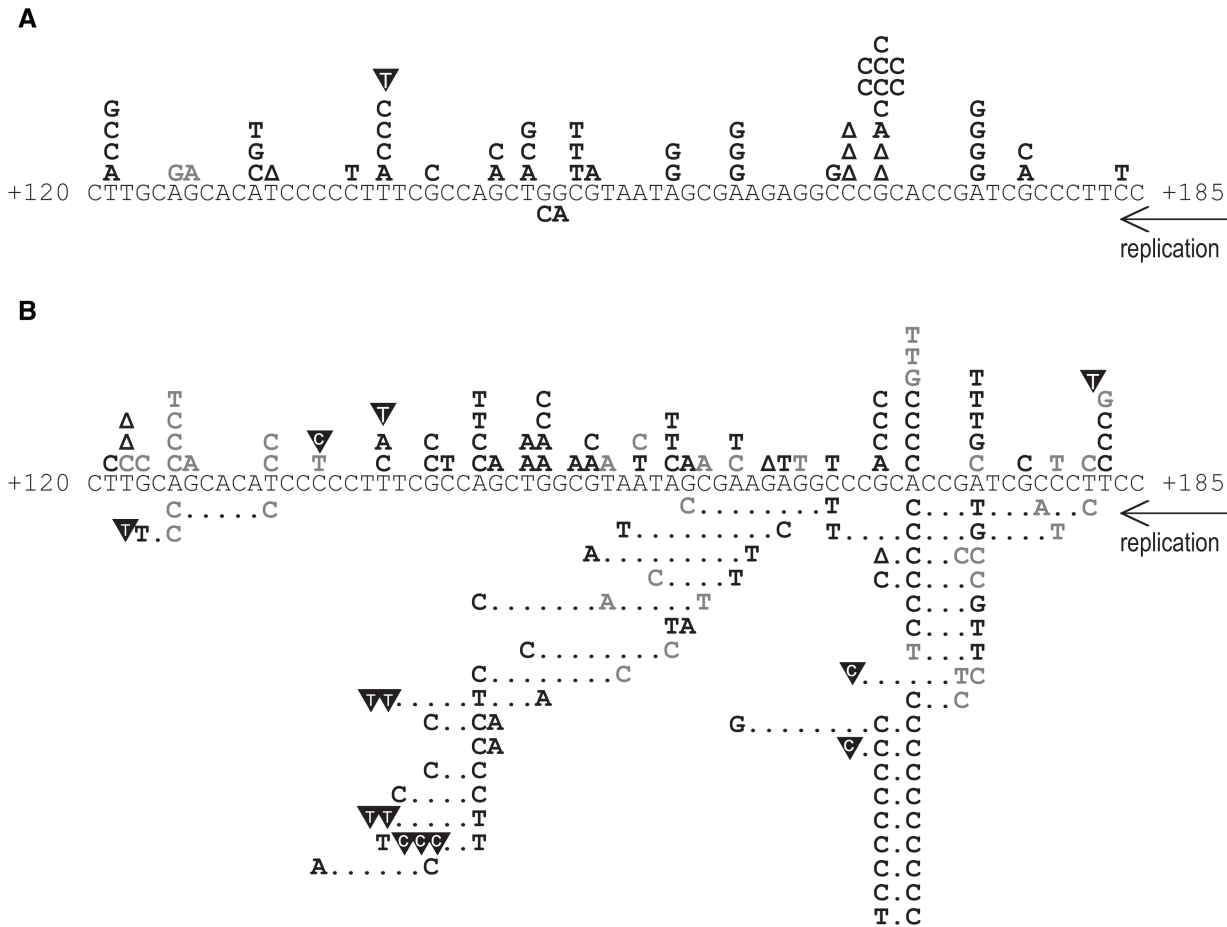


**Figure 5.** Spectra of mutations generated by wild-type and L979F Pol  $\zeta$ . Mutation spectra for a portion of the *lacZ* template (positions +120 through +185) in the (+) strand orientation are shown for (A) wild-type Pol  $\zeta$  in the presence of the accessory proteins and (B) L979F Pol  $\zeta$  in the presence of the accessory proteins. This portion of *lacZ* template was chosen because it contains the strongest hotspot for complex mutations generated by L979F Pol  $\zeta$ . The sequence is of the template strand and the direction of replication is indicated by the arrows. Single mutations are shown above the template and complex mutations and tandem base substitutions are shown below the template. Phenotypically detectable mutations are shown in black and undetectable mutations are shown in gray. Mutation types are indicated using letters for base substitutions, open triangles for  $-1$  deletions and inverted filled triangles for  $+1$  insertions. Unchanged bases within complex mutations are indicated with dots. Mutation spectra for the entire template can be found in Supplementary Figures 2 and 3.

a hotspot for single mutations, it likely that the local sequence context may to some extent affect whether L979F Pol  $\zeta$  reduces a single mutation or multiple closely spaced mutations.

## DISCUSSION

### Catalytic activity

Our previous genetic study predicted that a phenylalanine substitution for Leu-979 would not have a strong effect on the catalytic activity of Pol  $\zeta$ , because *rev3-L979F* haploid yeast retained nearly wild-type sensitivity to killing by UV light (43). Here we confirm this prediction and demonstrate that the processivity of L979F Pol  $\zeta$  is similar to that of wild-type Pol  $\zeta$  (Figure 2B and D), indicating that sequence-dependent interactions of L979F Pol  $\zeta$  with the primer-template are nearly normal. Similar retention of significant catalytic activity was reported for

substitutions at the homologous residues of RB69 Pol, yeast Pol  $\alpha$ ,  $\delta$  and  $\epsilon$ , and human Pol  $\alpha$  (31,35–40). These observations are consistent with the crystal structure of L415F RB69 Pol with a correct dNTP bound, which shows that the phenylalanine substitution does not perturb the geometry of the nascent base-pair binding pocket within the polymerase active site (38).

Previous studies have suggested that the sliding clamp PCNA can recruit Pol  $\zeta$  to sites of DNA damage, even though Pol  $\zeta$  lacks the consensus PCNA-binding motif present in many DNA polymerases and DNA repair proteins. However, while PCNA was found to stimulate TLS by Pol  $\zeta$  opposite UV-induced DNA lesions, PCNA had little effect on synthesis by Pol  $\zeta$  opposite undamaged templates (44). Our primer extension assays are in agreement with those of Garg *et al.* (44), in that addition of PCNA, RFC and RPA to primer extension reactions did not affect the processivity or termination probabilities of wild-type or L979F Pol  $\zeta$  when copying an undamaged

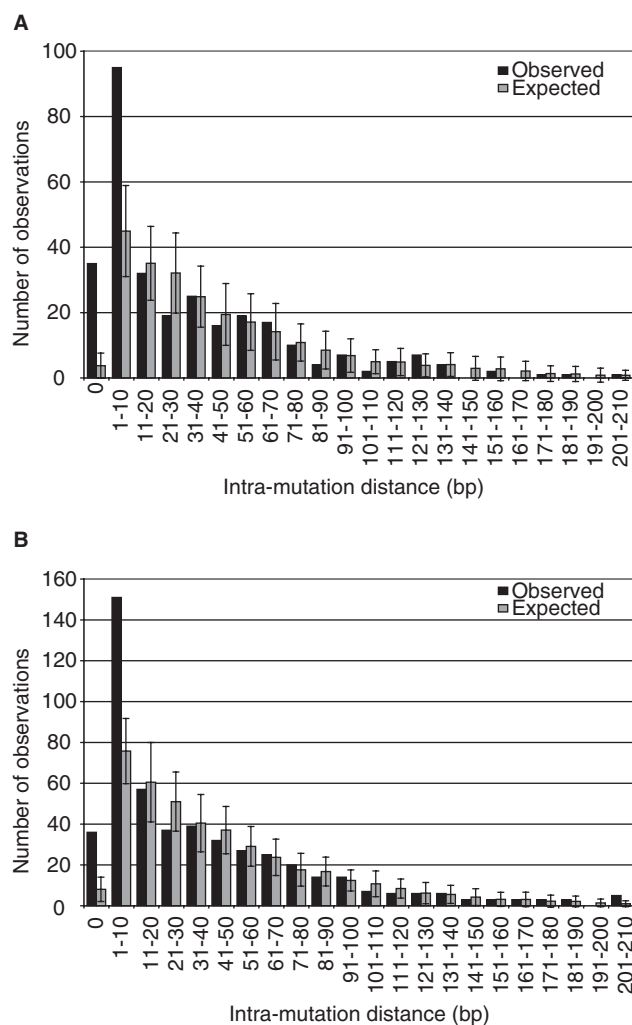


**Figure 6.** Distances between adjacent mutations created by L979F Pol  $\zeta$ . This figure shows the number of nucleotides between each pair of adjacent mutations identified from a single *lacZ* isolate for (A) the (+) strand template and (B) the (-) strand template. The number of mutation distances determined for any given *lacZ* isolate was  $N - 1$ , when  $N$  is the number of mutations identified in that isolate. Because adjacent mutations with zero intervening nucleotides may be produced in a single mutation event, these are considered as a separate class. If the one of the adjacent mutations was an insertion or deletion within a homopolymeric run, the distance from the outermost nucleotide of the run to the adjacent mutation was used. For example, a change of TTTCGCCAGCTG to TTTTTCGCCTGCTA (mutated bases are underlined) was considered to have 4 and 3 intervening nucleotides. Both phenotypically detectable and undetectable mutations were used in this analysis. Black bars represent observed values for each class. Gray bars indicate expected values for each class, which were generated by running 50 Monte Carlo simulations (see Supplementary Data for details) of 104 sequences for the (+) strand (5650 total mutations; average of 423 mutations per set) and 50 Monte Carlo simulations of 113 sequences for the (-) strand template (5200 total mutations; average of 250 mutations per set). Error bars for expected values represent 95% confidence intervals.

template (Figure 2B and D). However, the ability of wild-type and L979F Pol  $\zeta$  to cycle to new substrate molecules was reduced in the presence of the accessory proteins (Figure 2C), suggesting that while PCNA may be involved in the recruitment of Pol  $\zeta$ , additional factors may be required to remove Pol  $\zeta$  from DNA so that it can be

recycled to perform TLS elsewhere. Because Rev1 is thought to promote TLS *in vivo* via interactions with the Rev7 subunit of Pol  $\zeta$  (56,57) and PCNA (58), studies to assess the effects of Rev1 on the activity and fidelity of Pol  $\zeta$  are currently underway.

#### Error specificity for single-base substitutions

While L979F Pol  $\zeta$  retains catalytic activity, it has reduced DNA synthesis fidelity *in vitro* compared to wild-type Pol  $\zeta$ . This property is consistent with the fact that the *rev3-L979F* allele increases the rates of spontaneous and UV-induced mutagenesis compared to wild type (43). The elevated base substitutions error rates of L979F Pol  $\zeta$  clearly reveal that the phenylalanine substitution reduces discrimination against misinsertion of incorrect dNTPs. This is consistent with kinetic studies showing that the equivalent L-to-F mutations in RB69 Pol and yeast Pol  $\alpha$  decrease misinsertion discrimination (37,38). It is also possible that L979F Pol  $\zeta$  is even more promiscuous for mismatch extension than wild-type Pol  $\zeta$ , which has already been shown to extend mismatches with efficiencies of  $10^{-1}$  to  $10^{-2}$  (20,23,24). Because L979F Pol  $\zeta$  increases the error rates of some mismatches more than others, with the strongest effects for mismatches created by misinsertion of purines (Figure 4 and Supplementary Figure 1), it is possible that both misinsertion discrimination and/or promiscuous mismatch extension may be compromised to different extents for each type of mismatch. Finally, the variations in the locations (Figure 5) and rates of base substitutions between the (+) strand template and the (-) strand template (Figure 4 and Supplementary Figure 1) suggests that different neighboring sequences may affect fidelity when copying the two complementary strands of DNA. Regardless of the relative contributions of misinsertion discrimination, mismatch extension and sequence-context-dependent effects, the result is that L979F Pol  $\zeta$  produces error rates that are particularly high for misinsertion of purines (Figure 4 and Supplementary Figure 1). As a result, for most of the pairs of complementary mismatches that could account for a particular base substitution *in vivo* when complementary strands are replicated, L979F Pol  $\zeta$  is biased for creating the mismatch that involves misinsertion of a purine rather than the complementary misinsertion of a pyrimidine (Figure 4 and Supplementary Figure 1). As discussed below, this property of L979F Pol  $\zeta$  may be useful in tracking Pol  $\zeta$  function *in vivo*.

#### Complex mutations

A number of polymerases have been found to generate complex mutations at a high frequency *in vitro*, including yeast Pol  $\zeta$ , as well as human Pol  $\beta$  and Pol  $\theta$  (16,59,60). Wild-type Pol  $\zeta$  has also been found to generate complex mutations *in vivo* (6,7,17–19). L979F Pol  $\zeta$  generates *lacZ* mutants with two to five changes at significantly higher frequencies than predicted if these changes were generated independently (Supplementary Table 1). When the number of nucleotides between pairs of adjacent mutations was examined, mutations having 1–10 intervening nucleotides significantly exceeded the number predicted

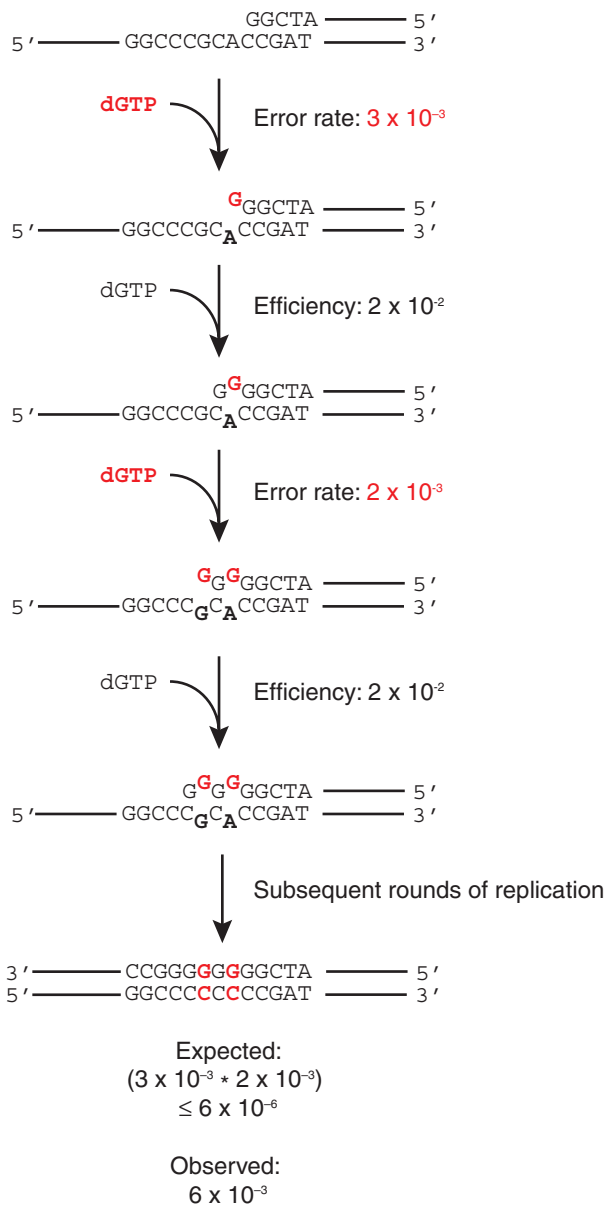


**Figure 7.** Model for generation of complex mutations by L979F Pol  $\zeta$ . This figure illustrates the events required to produce the complex mutation generated by L979F Pol  $\zeta$  at (+) strand position +176 (steps explained in text). Error rates shown for misincorporation events are for single A-to-C transversions generated by L979F Pol  $\zeta$  at these positions (Figure 4A). Efficiencies of extension from each mismatch are from kinetic studies of wild-type yeast Pol  $\zeta$  (GST-Rev3/Rev7) by Johnson *et al.* (22). The observed frequency of the complex mutation shown was calculated by dividing the number of complex events observed by the number mutants sequenced, multiplied by the mutant frequency.

by Monte Carlo simulations (Figure 6). Both facts indicate that L979F Pol  $\zeta$  generates closely spaced sequence changes more often than would be predicted by independent single-base polymerization errors. This suggests that the substitution of phenylalanine for Leu-979 exacerbates the inherent propensity of Pol  $\zeta$  for the generation of multiple, closely spaced mutations. In considering the mechanism responsible for the high rate of complex

mutations produced by Pol  $\zeta$  and L979F Pol  $\zeta$ , note that the distribution of closely spaced mutations in Figure 6 correlates with processivity, as each enzyme processively synthesizes 10-nucleotide patches and is capable of processive synthesis of at least 40 nucleotides (Figure 2B). This correlation and structural data for RB96 Pol (30) imply that a mismatch located between one and nine nucleotides upstream of the active site increases the rate at which the polymerase generates a second error during processive elongation. L979F Pol  $\zeta$  generates such complex mutations at frequencies that are much higher than would be predicted based on the mutation rates for single mutations alone. As one example, consider the most frequently observed complex mutation generated by L979F Pol  $\zeta$ . This event was observed 8 times among the 106 *lacZ* mutants that were sequenced (Supplementary Table 2). It involved an ACG to CCC change starting at position +176 of the (+) strand template. To generate this mutation (Figure 7), L979F Pol  $\zeta$  first misinserts dGTP opposite the template A, resulting in an A•dGMP mismatch. It then extends from this mismatch by inserting correct dGTP opposite the next template C. This is followed by misinsertion of dGTP opposite the next template G, and then mismatch extension is again required. This series of four unlikely events created the complex mutation at a rate at least 1000-fold higher than predicted by the error rates for individual A-to-C and G-to-C mutations at the same two template positions (Figure 7, bottom). This suggests that a perturbation in the duplex DNA upstream of the Pol  $\zeta$  active site greatly reduces the fidelity of replication for up to nine subsequent template bases. This idea was previously invoked to explain clustered single-base errors made by HIV-1 reverse transcriptase *in vitro* that are driven by dNTP pool imbalances (61). It was also invoked to explain Pol  $\zeta$ -dependent hotspots for complex mutations observed *in vivo*, in spectra obtained from the *lys2ΔA746* reporter that selects for reversion via +1 frameshifts (18). The authors of the latter study suggested that the first misinsertion might occur at a site of endogenous DNA damage to which Pol  $\zeta$  is recruited, leading to misinsertion followed by strand slippage to generate a single-base insertion.

#### Potential use of L979F Pol $\zeta$ to probe Pol $\zeta$ functions *in vivo*

The L979F Pol  $\zeta$  error signature described here should be distinctive enough to track the role of Pol  $\zeta$  in mutagenic synthesis *in vivo*. For example, certain single-base mismatches (e.g. G•dGMP) are generated at higher rates than are the complementary mismatches (e.g. C•dCMP) that could explain a base substitution (e.g. a G•C to C•G transversion) *in vivo*. This type of bias has been used to infer the identity of the major leading and lagging strand DNA polymerases in yeast (31,36,40). In a similar manner, the *rev3-L979F* allele could be useful to determine the contribution of Pol  $\zeta$  to strand-specific TLS (62,63) and to transcription-coupled mutagenesis *in vivo* (64). Indeed, we already found that *rev3-L979F* and *rev3-L979F rad30Δ* strains have elevated rates of UV-induced and spontaneous mutagenesis, suggesting that L979F Pol  $\zeta$  can bypass UV-induced and endogenous

DNA lesions in a mutagenic manner (43). These possibilities are currently being tested using purified L979F Pol  $\zeta$ .

Unlike most other polymerases, L979F Pol  $\zeta$  generates tandem double-base substitutions at a high frequency, and it generates complex mutations at an even higher frequency (Table 1). Complex mutations have already successfully been used to track wild-type Pol  $\zeta$  function in previous studies of strand-specific and sequence context specific TLS *in vivo* using a +1 frameshift reversion reporter system (6,7,17–19). Because L979F Pol  $\zeta$  generates complex mutations at a frequency that is even greater than wild-type Pol  $\zeta$ , it may be particularly useful in assays that require analysis of forward mutation reporters. This idea is supported by our previous genetic study, in which the numbers of complex mutations identified in the mutation spectra from both spontaneous and UV-induced *can1* mutants isolated from a *rev3-L979F* yeast strain were significantly higher than those isolated from the *REV3* strain (43). By extension, the generation of tandem double and/or complex mutations by L979F Pol  $\zeta$  may prove useful in studies of the Pol  $\zeta$ -dependent processes that require DNA synthesis to fill single-stranded gaps, including the repair of intrastrand crosslinks, gap-filling following replication past lesions, and recombination. Finally, studying mammalian Pol  $\zeta$  function *in vivo* is problematic because knocking out Pol  $\zeta$  function in mice results in embryonic lethality (65–67). The fact that yeast L979F Pol  $\zeta$  remains active as a polymerase and only modestly increases mutation rates and thereby may avoid error catastrophe, suggests that mice bearing a homozygous L-to-F missense allele of mouse Pol  $\zeta$  could be viable. If so, studies of this missense allele of Pol  $\zeta$  in mice could further our understanding of the contribution of mammalian Pol  $\zeta$  to spontaneous and damage-induced mutagenesis, somatic hypermutation (14,15) and possibly the origins of cancer.

## SUPPLEMENTARY DATA

Supplementary Data are available at NAR Online.

## ACKNOWLEDGEMENTS

We thank Jan Drake, Marilyn Diaz and Mercedes Arana for helpful discussions, Stephanie Nick McElhinny and Dinh Nguyen for creation and preparation of gapped substrates, and the NIEHS DNA Sequencing Facility and the NIEHS Molecular Genetics Core for their assistance.

## FUNDING

National Institutes of Health (GM032431 to P.M.J.B, partial.); Intramural Research Program of the National Institutes of Health, National Institute of Environmental Health Sciences (Project Z01 ES065070 to T.A.K, partial.); Intramural Research Program of the National Institutes of Health, National Library of Medicine (to I.B.R., partial). Funding for open access charge: Intramural Research Program of the National Institutes

of Health, National Institute of Environmental Health Sciences, Project Z01 ES065070 to T.A.K..

*Conflict of interest statement.* None declared.

## REFERENCES

- Lawrence,C.W. (2004) Cellular functions of DNA polymerase zeta and Rev1 protein. *Adv. Protein Chem.*, **69**, 167–203.
- Gan,G.N., Wittschieben,J.P., Wittschieben,B.O. and Wood,R.D. (2008) DNA polymerase zeta (pol zeta) in higher eukaryotes. *Cell Res.*, **18**, 174–183.
- Lawrence,C.W., Das,G. and Christensen,R.B. (1985) *REV7*, a new gene concerned with UV mutagenesis in yeast. *Mol. Gen. Genet.*, **200**, 80–85.
- Lawrence,C.W., Nisson,P.E. and Christensen,R.B. (1985) UV and chemical mutagenesis in *rev7* mutants of yeast. *Mol. Gen. Genet.*, **200**, 86–91.
- Lemontt,J.F. (1971) Mutants of yeast defective in mutation induced by ultraviolet light. *Genetics*, **68**, 21–33.
- Minesinger,B.K., Abdulovic,A.L., Ou,T.M. and Jinks-Robertson,S. (2006) The effect of oxidative metabolism on spontaneous Pol zeta-dependent translesion synthesis in *Saccharomyces cerevisiae*. *DNA Repair*, **5**, 226–234.
- Minesinger,B.K. and Jinks-Robertson,S. (2005) Roles of RAD6 epistasis group members in spontaneous pol zeta-dependent translesion synthesis in *Saccharomyces cerevisiae*. *Genetics*, **169**, 1939–1955.
- Quah,S.K., von Borstel,R.C. and Hastings,P.J. (1980) The origin of spontaneous mutation in *Saccharomyces cerevisiae*. *Genetics*, **96**, 819–839.
- Sabbioneda,S., Minesinger,B.K., Giannattasio,M., Plevani,P., Muzi-Falconi,M. and Jinks-Robertson,S. (2005) The 9-1-1 checkpoint clamp physically interacts with pol zeta and is partially required for spontaneous pol zeta-dependent mutagenesis in *Saccharomyces cerevisiae*. *J. Biol. Chem.*, **280**, 38657–38665.
- Holbeck,S.L. and Strathern,J.N. (1997) A role for *REV3* in mutagenesis during double-strand break repair in *Saccharomyces cerevisiae*. *Genetics*, **147**, 1017–1024.
- Ratray,A.J., Shafer,B.K., McGill,C.B. and Strathern,J.N. (2002) The roles of *REV3* and *RAD57* in double-strand-break-repair-induced mutagenesis of *Saccharomyces cerevisiae*. *Genetics*, **162**, 1063–1077.
- Raschle,M., Knipsheer,P., Enoiu,M., Angelov,T., Sun,J., Griffith,J.D., Ellenberger,T.E., Schärer,O.D. and Walter,J.C. (2008) Mechanism of replication-coupled DNA interstrand crosslink repair. *Cell*, **134**, 969–980.
- Sarkar,S., Davies,A.A., Ulrich,H.D. and McHugh,P.J. (2006) DNA interstrand crosslink repair during G1 involves nucleotide excision repair and DNA polymerase zeta. *EMBO J.*, **25**, 1285–1294.
- Diaz,M. and Lawrence,C. (2005) An update on the role of translesion synthesis DNA polymerases in Ig hypermutation. *Trends Immunol.*, **26**, 215–220.
- Diaz,M., Verkoczy,L.K., Flajnik,M.F. and Klinman,N.R. (2001) Decreased frequency of somatic hypermutation and impaired affinity maturation but intact germinal center formation in mice expressing antisense RNA to DNA polymerase zeta. *J. Immunol.*, **167**, 327–335.
- Zhong,X., Garg,P., Stith,C.M., Nick McElhinny,S.A., Kissling,G.E., Burgers,P.M. and Kunkel,T.A. (2006) The fidelity of DNA synthesis by yeast DNA polymerase zeta alone and with accessory proteins. *Nucleic Acids Res.*, **34**, 4731–4742.
- Abdulovic,A.L. and Jinks-Robertson,S. (2006) The *in vivo* characterization of translesion synthesis across UV-induced lesions in *Saccharomyces cerevisiae*: insights into Pol zeta- and Pol eta-dependent frameshift mutagenesis. *Genetics*, **172**, 1487–1498.
- Harfe,B.D. and Jinks-Robertson,S. (2000) DNA polymerase zeta introduces multiple mutations when bypassing spontaneous DNA damage in *Saccharomyces cerevisiae*. *Mol. Cell*, **6**, 1491–1499.
- Northam,M.R., Garg,P., Baitin,D.M., Burgers,P.M. and Shcherbakova,P.V. (2006) A novel function of DNA polymerase zeta regulated by PCNA. *EMBO J.*, **25**, 4316–4325.

20. Johnson, R.E., Yu, S.L., Prakash, S. and Prakash, L. (2003) Yeast DNA polymerase zeta (zeta) is essential for error-free replication past thymine glycol. *Genes Dev.*, **17**, 77–87.
21. Nelson, J.R., Lawrence, C.W. and Hinkle, D.C. (1996) Thymine-thymine dimer bypass by yeast DNA polymerase zeta. *Science*, **272**, 1646–1649.
22. Johnson, R.E., Washington, M.T., Haracska, L., Prakash, S. and Prakash, L. (2000) Eukaryotic polymerases iota and zeta act sequentially to bypass DNA lesions. *Nature*, **406**, 1015–1019.
23. Lawrence, C.W., Gibbs, P.E., Murante, R.S., Wang, X.D., Li, Z., McManus, T.P., McGregor, W.G., Nelson, J.R., Hinkle, D.C. and Maher, V.M. (2000) Roles of DNA polymerase zeta and Rev1 protein in eukaryotic mutagenesis and translesion replication. *Cold Spring Harb. Symp. Quant. Biol.*, **65**, 61–69.
24. Lawrence, C.W. and Hinkle, D.C. (1996) DNA polymerase zeta and the control of DNA damage induced mutagenesis in eukaryotes. In Lindahl, T. (ed.), *Cancer Surveys: Genetic Instability in Cancer*, Vol. 20, pp. 21–31.
25. Guo, D., Wu, X., Rajpal, D.K., Taylor, J.S. and Wang, Z. (2001) Translesion synthesis by yeast DNA polymerase zeta from templates containing lesions of ultraviolet radiation and acetylaminofluorene. *Nucleic Acids Res.*, **29**, 2875–2883.
26. Haracska, L., Prakash, L. and Prakash, S. (2003) A mechanism for the exclusion of low-fidelity human Y-family DNA polymerases from base excision repair. *Genes Dev.*, **17**, 2777–2785.
27. Haracska, L., Unk, I., Johnson, R.E., Johansson, E., Burgers, P.M., Prakash, S. and Prakash, L. (2001) Roles of yeast DNA polymerases delta and zeta and of Rev1 in the bypass of abasic sites. *Genes Dev.*, **15**, 945–954.
28. Johnson, R.E., Haracska, L., Prakash, S. and Prakash, L. (2001) Role of DNA polymerase eta in the bypass of a (6-4) TT photoproduct. *Mol. Cell Biol.*, **21**, 3558–3563.
29. Prakash, S. and Prakash, L. (2002) Translesion DNA synthesis in eukaryotes: a one- or two-polymerase affair. *Genes Dev.*, **16**, 1872–1883.
30. Franklin, M.C., Wang, J. and Steitz, T.A. (2001) Structure of the replicating complex of a pol alpha family DNA polymerase. *Cell*, **105**, 657–667.
31. Nick McElhinny, S.A., Gordenin, D.A., Stith, C.M., Burgers, P.M. and Kunkel, T.A. (2008) Division of labor at the eukaryotic replication fork. *Mol. Cell*, **30**, 137–144.
32. Beechem, J.M., Otto, M.R., Bloom, L.B., Eritja, R., Reha-Krantz, L.J. and Goodman, M.F. (1998) Exonuclease-polymerase active site partitioning of primer-template DNA strands and equilibrium Mg<sup>2+</sup> binding properties of bacteriophage T4 DNA polymerase. *Biochemistry*, **37**, 10144–10155.
33. Fidalgo da Silva, E., Mandal, S.S. and Reha-Krantz, L.J. (2002) Using 2-aminopurine fluorescence to measure incorporation of incorrect nucleotides by wild type and mutant bacteriophage T4 DNA polymerases. *J. Biol. Chem.*, **277**, 40640–40649.
34. Reha-Krantz, L.J. and Nonay, R.L. (1994) Motif A of bacteriophage T4 DNA polymerase: role in primer extension and DNA replication fidelity. Isolation of new antimutator and mutator DNA polymerases. *J. Biol. Chem.*, **269**, 5635–5643.
35. Li, L., Murphy, K.M., Kanevets, U. and Reha-Krantz, L.J. (2005) Sensitivity to phosphonoacetic acid: a new phenotype to probe DNA polymerase delta in *Saccharomyces cerevisiae*. *Genetics*, **170**, 569–580.
36. Nick McElhinny, S.A., Stith, C.M., Burgers, P.M. and Kunkel, T.A. (2007) Inefficient proofreading and biased error rates during inaccurate DNA synthesis by a mutant derivative of *Saccharomyces cerevisiae* DNA polymerase delta. *J. Biol. Chem.*, **282**, 2324–2332.
37. Niimi, A., Limsirichaikul, S., Yoshida, S., Iwai, S., Masutani, C., Hanaoka, F., Kool, E.T., Nishiyama, Y. and Suzuki, M. (2004) Palm mutants in DNA polymerases alpha and eta alter DNA replication fidelity and translesion activity. *Mol. Cell Biol.*, **24**, 2734–2746.
38. Zhong, X., Pedersen, L.C. and Kunkel, T.A. (2008) Characterization of a replicative DNA polymerase mutant with reduced fidelity and increased translesion synthesis capacity. *Nucleic Acids Res.*, **36**, 3892–3904.
39. Pursell, Z.F., Isoz, I., Lundstrom, E.B., Johansson, E. and Kunkel, T.A. (2007) Regulation of B family DNA polymerase fidelity by a conserved active site residue: characterization of M644W, M644L and M644F mutants of yeast DNA polymerase epsilon. *Nucleic Acids Res.*, **35**, 3076–3086.
40. Pursell, Z.F., Isoz, I., Lundstrom, E.B., Johansson, E. and Kunkel, T.A. (2007) Yeast DNA polymerase epsilon participates in leading-strand DNA replication. *Science*, **317**, 127–130.
41. Patel, P.H., Kawate, H., Adman, E., Ashbach, M. and Loeb, L.A. (2001) A single highly mutable catalytic site amino acid is critical for DNA polymerase fidelity. *J. Biol. Chem.*, **276**, 5044–5051.
42. Shinkai, A. and Loeb, L.A. (2001) In vivo mutagenesis by *Escherichia coli* DNA polymerase I. Ile(709) in motif A functions in base selection. *J. Biol. Chem.*, **276**, 46759–46764.
43. Sakamoto, A.N., Stone, J.E., Kissling, G.E., McCulloch, S.D., Pavlov, Y.I. and Kunkel, T.A. (2007) Mutator alleles of yeast DNA polymerase zeta. *DNA Repair*, **6**, 1829–1838.
44. Garg, P., Stith, C.M., Majka, J. and Burgers, P.M. (2005) Proliferating cell nuclear antigen promotes translesion synthesis by DNA polymerase zeta. *J. Biol. Chem.*, **280**, 23446–23450.
45. Fortune, J.M., Stith, C.M., Kissling, G.E., Burgers, P.M. and Kunkel, T.A. (2006) RPA and PCNA suppress formation of large deletion errors by yeast DNA polymerase delta. *Nucleic Acids Res.*, **34**, 4335–4341.
46. Ayyagari, R., Gomes, X.V., Gordenin, D.A. and Burgers, P.M. (2003) Okazaki fragment maturation in yeast. I. Distribution of functions between FEN1 AND DNA2. *J. Biol. Chem.*, **278**, 1618–1625.
47. Henricksen, L.A., Umbricht, C.B. and Wold, M.S. (1994) Recombinant replication protein A: expression, complex formation, and functional characterization. *J. Biol. Chem.*, **269**, 11121–11132.
48. McCulloch, S.D., Wood, A., Garg, P., Burgers, P.M. and Kunkel, T.A. (2007) Effects of accessory proteins on the bypass of a cis-syn thymine-thymine dimer by *Saccharomyces cerevisiae* DNA polymerase eta. *Biochemistry*, **46**, 8888–8896.
49. Bebenek, K. and Kunkel, T.A. (1989) The use of native T7 DNA polymerase for site-directed mutagenesis. *Nucleic Acids Res.*, **17**, 5408.
50. Bebenek, K. and Kunkel, T.A. (1995) Analyzing fidelity of DNA polymerases. *Methods Enzymol.*, **262**, 217–232.
51. Rogozin, I.B., Kondrashov, F.A. and Glazko, G.V. (2001) Use of mutation spectra analysis software. *Hum. Mutation*, **17**, 83–102.
52. Rogozin, I.B., Pavlov, Y.I., Bebenek, K., Matsuda, T. and Kunkel, T.A. (2001) Somatic mutation hotspots correlate with DNA polymerase eta error spectrum. *Nat. Immunol.*, **2**, 530–536.
53. McCulloch, S.D., Kokoska, R.J., Garg, P., Burgers, P.J.M. and Kunkel, T.A. (2009) The efficiency and fidelity of 8-oxo-guanine bypass by DNA polymerases delta and eta. *Nucleic Acids Res.*, in press.
54. Drake, J.W., Bebenek, A., Kissling, G.E. and Peddada, S. (2005) Clusters of mutations from transient hypermutability. *Proc. Natl Acad. Sci. USA*, **102**, 12849–12854.
55. Garcia-Diaz, M. and Kunkel, T.A. (2006) Mechanism of a genetic glissando: structural biology of indel mutations. *Trends Biochem. Sci.*, **31**, 206–214.
56. D'Souza, S. and Walker, G.C. (2006) Novel role for the C terminus of *Saccharomyces cerevisiae* Rev1 in mediating protein-protein interactions. *Mol. Cell Biol.*, **26**, 8173–8182.
57. Acharya, N., Johnson, R.E., Prakash, S. and Prakash, L. (2006) Complex formation with Rev1 enhances the proficiency of *Saccharomyces cerevisiae* DNA polymerase zeta for mismatch extension and for extension opposite from DNA lesions. *Mol. Cell Biol.*, **26**, 9555–9563.
58. Guo, C., Sonoda, E., Tang, T.S., Parker, J.L., Bielen, A.B., Takeda, S., Ulrich, H.D. and Friedberg, E.C. (2006) REV1 protein interacts with PCNA: significance of the REV1 BRCT domain in vitro and in vivo. *Mol. Cell*, **23**, 265–271.
59. Arana, M.E., Seki, M., Wood, R.D., Rogozin, I.B. and Kunkel, T.A. (2008) Low-fidelity DNA synthesis by human DNA polymerase theta. *Nucleic Acids Res.*, **36**, 3847–3856.
60. Osheroff, W.P., Beard, W.A., Wilson, S.H. and Kunkel, T.A. (1999) Base substitution specificity of DNA polymerase beta depends on interactions in the DNA minor groove. *J. Biol. Chem.*, **274**, 20749–20752.

61. Bebenek, K., Roberts, J.D. and Kunkel, T.A. (1992) The effects of dNTP pool imbalances on frameshift fidelity during DNA replication. *J. Biol. Chem.*, **267**, 3589–3596.
62. Abdulovic, A.L., Minesinger, B.K. and Jinks-Robertson, S. (2007) Identification of a strand-related bias in the PCNA-mediated bypass of spontaneous lesions by yeast Pol  $\epsilon$ . *DNA Repair*, **6**, 1307–1318.
63. Yang, Y., Sterling, J., Storici, F., Resnick, M.A. and Gordenin, D.A. (2008) Hypermutability of damaged single-strand DNA formed at double-strand breaks and uncapped telomeres in yeast *Saccharomyces cerevisiae*. *PLoS Genet.*, **4**, e1000264.
64. Datta, A. and Jinks-Robertson, S. (1995) Association of increased spontaneous mutation rates with high levels of transcription in yeast. *Science*, **268**, 1616–1619.
65. Bemark, M., Khamlichi, A.A., Davies, S.L. and Neuberger, M.S. (2000) Disruption of mouse polymerase zeta (Rev3) leads to embryonic lethality and impairs blastocyst development in vitro. *Curr. Biol.*, **10**, 1213–1216.
66. Wittschieben, J., Shivji, M.K., Lalani, E., Jacobs, M.A., Marini, F., Gearhart, P.J., Rosewell, I., Stamp, G. and Wood, R.D. (2000) Disruption of the developmentally regulated Rev3l gene causes embryonic lethality. *Curr. Biol.*, **10**, 1217–1220.
67. Esposito, G., Godindagger, I., Klein, U., Yaspo, M.L., Cumano, A. and Rajewsky, K. (2000) Disruption of the Rev3l-encoded catalytic subunit of polymerase zeta in mice results in early embryonic lethality. *Curr. Biol.*, **10**, 1221–1224.